IEEE Access
Multidisciplinary ⋮ Rapid Review ⋮ Open Access Journal

Received October 26, 2021, accepted November 4, 2021, date of publication November 8, 2021,
date of current version November 22, 2021.

Digital Object Identifier 10.1109/ACCESS.2021.3126667

Design and Analysis of a Novel Mechanic-Electronic-Hydraulic Powertrain System for Agriculture Tractors

ZHEN ZHU[1,2], (Member, IEEE), LONGHUI LAI[1], (Member, IEEE), XIAODONG SUN[1,2], (Senior Member, IEEE), LONG CHEN[1], (Member, IEEE), AND YINGFENG CAI[1], (Member, IEEE)

[1]Automotive Engineering Research Institute, Jiangsu University, Zhenjiang 212013, China
[2]State Key Laboratory of Automotive Simulation and Control, Jilin University, Changchun 130025, China

Corresponding author: Yingfeng Cai (caicaixiao0304@126.com)

This work was supported in part by the National Natural Science Foundation of China under Grant 51805222, Grant 51875255, and Grant U20A20331; in part by the Open Fund of State Key Laboratory of Automotive Simulation and Control under Grant 20201201; and in part by the Project of Jiangsu Provincial Six Talent Peaks under Grant 2018-TD-GDZB-022.

ABSTRACT This paper introduces a mechanic-electronic-hydraulic powertrain system (MEH-PS) composed of an electro-mechanical hybrid system and hydro-mechanical composite transmission according to current mainstream drive and transmission technologies. Firstly, the structural design concept of the system is introduced, and the power and transmission components are selected according to the actual working requirements of the tractor. Then, the principles of various drive modes and transmission modes of the powertrain system are explained, and the speed regulation characteristic curves of the hydro-mechanical transmission (HMT) are given; the speed characteristics, torque characteristics, power split characteristics, and efficiency characteristics of the powertrain system are analyzed. Finally, a tractor simulation and test model was developed to verify its performance under certain operating conditions. Simulation results show that: the tractor acceleration performance is improved, the speed range is wider, the power components and hydraulic components can also meet the requirements, the HMT in a wide range of speed to maintain the average efficiency of above 86%. The bench test results show that: the step-less speed regulation characteristics and efficiency characteristics of the powertrain system are basically consistent with the simulation results.

INDEX TERMS Agriculture tractors, performance study, hybrid system, hydro-mechanical transmission (HMT), powertrain design.

NOMENCLATURE

F_t	wheel driving force [kN]
F_f	rolling resistance [kN]
F_i	ramp resistance [kN]
F_a	air resistance [kN]
F_j	acceleration resistance [kN]
F_T	hook tension [kN]
Z_x	number of the ploughshare
B_x	monomer ploughshare width [m]
H_x	ploughing depth [m]
K_x	soil specific resistance [N/cm^2]
P_e	rated power of diesel engine [kW]
P_m	rated power of electric motor [kW]
ΔP_{Pmax}	maximum pressure of pump [bar]
$Q_{P\,max}$	maximum flow rate of pump [L/min]
v	tractor speed [km/h]
n_e	rated speed of engine [rpm]
T_e	output torque of engine[N·m]
n_m	rated speed of motor [rpm]
T_m	output torque of motor [N·m]
K	planetary gear set
G	fixed shaft gear set
e	displacement ratio
i_g	gear ratio of transmission
$k_1 \sim k_4$	characteristic parameter of the planetary gear set $K_1 \sim K_4$

The associate editor coordinating the review of this manuscript and approving it for publication was Jie Gao.

i_{st}	transmission ratio the sub-transmission
i_1	transmission ratio of engine and pump
i_2	fixed-displacement motor gear ratio
MEH-PS	mechanic-electronic-hydraulic powertrain system
HMT	hydro-mechanical transmission
CVT	continuously variable transmission
ICE	internal combustion engine
MG	motor-generator
PTO	power take-off
TC	torque coupling
SC	speed coupling
DOH	degree of hybridization
VDP	variable displacement pump
FDM	fixed-displacement motor

GREEK LETTERS

η_T	traction efficiency
β	overload capacity coefficient
η_P	efficiency of pump
η_M	efficiency of motor
ρ	power split ratio
φ	planetary gear power loss coefficient
η_t	transmission efficiency

SUBSCRIPT AND SUPERSCRIPTS

in	input shaft
out	output shaft
s	sun gear of the planetary gear set
c	carrier of the planetary gear set
r	ring gear of the planetary gear set

I. INTRODUCTION

There are two important research trends for vehicle powertrain nowadays, one is to improve the performance of the transmission to meet the driving needs for vehicles based on traditional power sources, such as the continuously variable transmission (CVT) which has been widely used in recent years to make the engine have the optimal power output under different working conditions [1], [2]. Another trend is to study the coordinated work of power sources, such as overcoming the shortcomings of single power source operation by a dual power source consisting of an engine and an electric motor [3], with motor assistance to fill the load not covered by the engine, while improving the economic performance of the system [4].

Tractors work in a variety of operations, When performing farm operations, they need to provide greater traction [5]; when performing road transportation, they have high requirements of tractor speed [6]. To meet these requirements, tractors equipped with stepped transmissions provide speed ratios for different speeds and drive force needs by adding extra gears, but this also makes the structure and operation of the transmission complex [7], [8]. HMT has the CVT feature which is suitable for agricultural and construction machinery [9], [10]. Due to its large speed ratio range, compared with traditional tractors, the number of gears is significantly reduced, the space structure is optimized, and the weight of the whole machine is reduced [11]. Furthermore, the driving comfort of the tractor is improved as a result of fewer gears and avoidance of frequent gear shifts [12].

The hydro-mechanical transmission developed by Fendt splits power through planetary gear, eliminating the necessity of complex multi-gear transmission and allowing the tractor to be continuously shifted over a wide speed range by simply controlling the swing angle of the pump and motor (0∼45°) [13], but the dual-variable hydraulic scomponents are technically challenging and expensive to promote [14]. The 4-planetary gears hydro-mechanical transmission developed by Steyr can output variable speed at constant engine speed and achieve step-less speed regulation of the forward and reverse 0-50 km/h speed range without power interruption, but the multi-planetary gears structure convergence and shift control strategy are complex [15]. Liu *et al.* proposed a multi-speed HMT with a two-stage input coupling layout, in which the maximum speed of the vehicle can be significantly increased by changing the two-phase (positive and negative) power split of the hydrostatic circuit, but the device suffers from low efficiency in multiple speed ranges [16]. Wang *et al.* designed a single planetary HMT, which has a simplified structure compared to a multi-planetary transmission but has a limited speed range to meet the increasing speed requirements of tractors [17].

Toyota Hybrid System (THS) achieves a multi-coupling output of the engine and motor power through planetary gears and fixed shaft gears, enabling the vehicle to meet both comfort and power requirements in different operating modes, and the multi-coupling approach gives more degrees of freedom to the powertrain, more flexible torque and speed adjustment, and a significant vehicle performance improvement [18]. Joshi investigated the planetary gear and shaft fixed-gear mechanism to develop a hybrid powertrain with torque coupling and speed coupling. This powertrain can decouple the engine speed and torque from the vehicle drive wheels without the need for a complex transmission, and the engine can operate within its efficient speed and torque range to obtain greater drive torque and drive speed with the assistance of an electric motor, while the fuel consumption of the vehicle is lower [19], [20]. Mocera and Somà studied the application of an electro-mechanical hybrid system in tractors, which can lower the engine specifications with the assistance of electric motors while satisfying the whole tractor operation [21]. Moreda's *et al.* research points out that a hybrid power system allows more freedom of torque and speed control of the tractor while reducing noise [22].

There is no research on combining electromechanical hybrids with HMT in the field of tractors or other vehicles till now. The application of this technology in tractors seems to be promising given the application of road vehicles, as the dual power source has additional degrees of freedom, which can simplify the structure of transmission to

some extent while lowering the requirements for transmission component specifications. Combining the design ideas of the above scheme and proposes a MEH-PS for tractors. This paper firstly analyzes the design concept of the powertrain, then analyzes its speed characteristics, torque characteristics, power split, and efficiency characteristics, finally, verify the theoretical analysis results through simulation and test bench.

II. DESIGN CONCEPT

A. DESIGN CONCEPT OF THE SCHEME

The design concept of the MEH-PS proposed in this paper is shown in Fig 1, the structure has two power sources: internal combustion engine (ICE) and motor-generator (MG), both of which can output power individually or simultaneously.

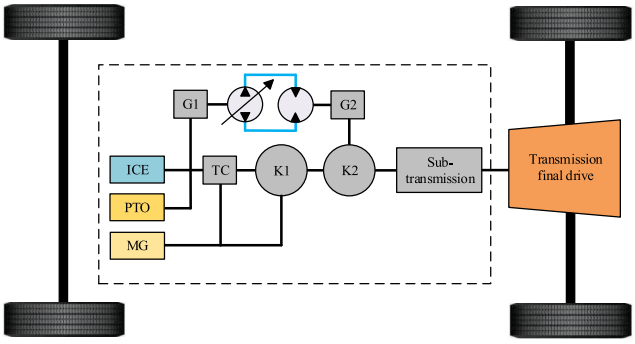

FIGURE 1. MEH-PS structure principle.

When the tractor is operating in the unloaded transit condition, the required power is low, the pure electric drive mode can meet the power requirements. When the tractor is operating in plowing condition, the pure engine drive mode is the main drive mode. When the required torque is high, such as the power take-off (PTO) output power or acceleration process can be driven through the torque coupling (TC) mode. When the required speed is high, through the K1 (1st planetary gear set) to achieve speed coupling (SC) mode. The motor can regulate the torque and speed of the drivetrain independently of the engine through TC mode and SC mode.

The hydraulic system input power is split through the G1 (fixed shaft gear set) and passes through G2 to merge with the power from the mechanical path in the K2. Considering that the hybrid system provides more degree of freedom, the structure uses only a single planetary gear set for power merging. The power can be outputted through hydrostatic transmission mode, hydro-mechanical transmission mode, or mechanical transmission mode as needed, and finally adjusted and outputted to the drive axle through the sub-transmission to drive the tractor forward or backward.

B. SCHEME REALIZATION

A MEH-PS with independent intellectual property rights for tractors was designed based on the above design concepts, and the details of the powertrain are shown in Fig 2.

C. MAIN COMPONENTS MATCHING

To facilitate the following analysis of the performance of the MEH-PS, the relevant parameters of the power source and transmission components need to be determined.

The longitudinal dynamics of tractors can be expressed by the following equation:

$$F_{\mathrm{t}} = F_{\mathrm{f}} + F_{\mathrm{i}} + F_{\mathrm{a}} + F_{\mathrm{j}} + F_{\mathrm{T}} \tag{1}$$

where, F_{t} is the wheel driving force, F_{f} is the rolling resistance, F_{i} is the ramp resistance, F_{a} is the air resistance, F_{j} is the acceleration resistance, and F_{T} is the hook tension.

Engine selection: the power required for tractor plowing operation is the highest under various operating conditions, and the hook tension during the plowing operation can be expressed by the following formula [23]:

$$F_{\mathrm{T}} = Z_x B_x H_x K_x \tag{2}$$

where Z_x is the number of the ploughshare, B_x is the monomer ploughshare, H_x is the ploughing depth, and K_x is soil specific resistance. The parameters of the tractor-matched 1LF-550 reversible plow are as follows: $Z_x = 5$, $B_x = 0.45$m, $H_x = 0.25$m, $K_x = 7\mathrm{N/cm}^2$; considering that the tractor needs a power reservation, according to the calculation: $F_{\mathrm{t\,max}} = 1.2F_{\mathrm{T}} = 47.25$kN.

Tractor plowing operation speed generally is 5∼10km/h, this paper selected for 7km/h, the traction efficiency of wheeled tractor generally is $\eta_{\mathrm{T}} = 0.7$, According to the above conditions, the engine rated power is calculated as $P_{\mathrm{e}} = F_{\mathrm{t\,max}} v / 3.6\eta_{\mathrm{T}} = 131.25$kW, after comparison, the WP6.180E40 diesel engine was selected to meet the requirements.

Motor selection: motor selection usually takes into account the degree of hybridization (DOH), which is the parameter of the percentage of the total power of the motor to the power source [24].

$$\mathrm{DOH} = \frac{P_{\mathrm{m}}}{P_{\mathrm{e}} + P_{\mathrm{m}}} \tag{3}$$

According to the data related to the tractors in operation, when the tractor is in transit or sowing and other low load operations, the required power of the whole tractor can be up to 50% [25], given the overload capacity of the motor $\beta = P_{\mathrm{m\,max}} / P_{\mathrm{m}} \geq 2$, the motor power is accounted for 25% of the whole tractor, it is calculated that the rated power of the motor is $P_{\mathrm{m}} = 45$kW. Considering the size of the motor and the need to expand the speed range of the tractor, the hybrid system tends to choose a high-speed motor, and the TZ205XS85K01 electric motor is selected after comparison. The specific parameters of power sources are shown in Table 1.

The selection of hydraulic components should be able to match the selected power source. The engine is the main power source of the tractor, therefore the parameters of the engine are mainly considered for matching [26]. The pump is connected to the engine and the relevant parameters of the

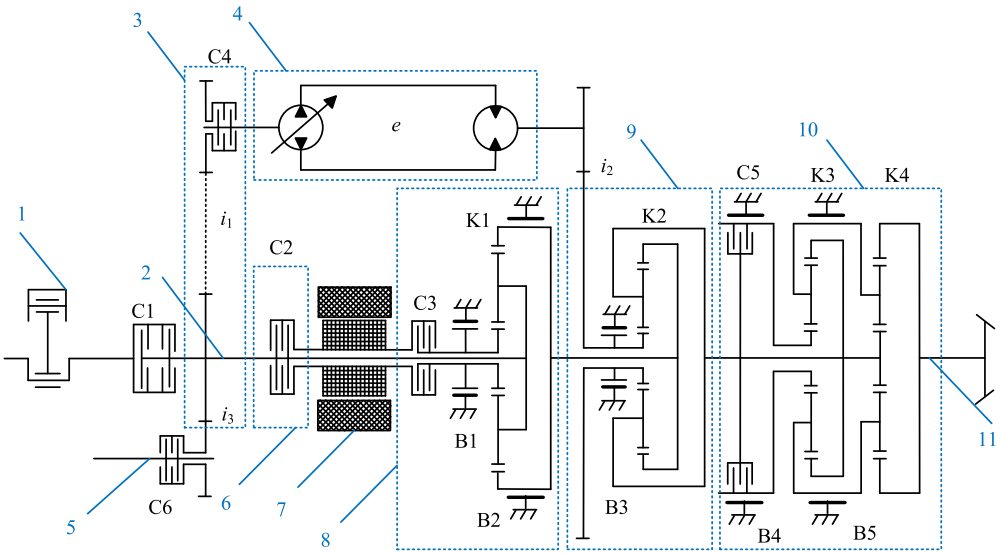

FIGURE 2. **Configuration Scheme. 1. ICE 2. Input shaft 3. Power split mechanism 4. Hydraulic system 5. PTO 6. TC mechanism 7. MG 8. SC mechanism 9. Power merging mechanism 10. Sub-transmission 11. Output shaft. C is the clutch, B is the brake, *e* is the displacement ratio, i_1, i_2 is the gear ratio.**

TABLE 1. **Power source parameters.**

Engine	Model	WP6.180E40
	Rated power	132kW
	Rated speed	2200rpm
	Maximum torque	750N·m
Motor	Model	TZ205XS85K01
	Rated (Maximum) power	45(95)kW
	Maximum torque	250 N·m
	Maximum speed	11000 rpm

hydraulic components should satisfy the following equation.

$$P_{\mathrm{P}\max} = \frac{Q_{\mathrm{P}\max}\Delta P_{\mathrm{P}\max}}{600\eta_{\mathrm{P}}} \geq P_{\mathrm{e}\max} \tag{4}$$

where $P_{\mathrm{P}\max}$ is the maximum pump power [kW]; $Q_{\mathrm{P}\max}$ is the maximum pump flow rate [L/min]; $\Delta P_{\mathrm{P}\max}$ is the maximum pump oil pressure [bar]; if the pump is in the case of maximum flow, the pump efficiency $\eta_{\mathrm{P}} = 0.95$, according to the parameter of SAUER_DANFOSS 90-series hydraulic components $\Delta P_{\mathrm{P}\max} = 480$bar, therefore $Q_{\mathrm{P}\max} \geq 156.7\mathrm{L}/\mathrm{min}$. Considering the cost-effectiveness and size for this study, 0-55 series variable displacement pump (VDP) and fixed-displacement motor (FDM) are suitable to selected [27], and the specific parameters of the hydraulic components are shown in Table 2.

III. OPERATING PRINCIPLES OF THE MEH-PS

A. DRIVE MODES ANALYSIS

The switching element engagement states of the four drive modes of the MEH-PS are shown in Table 3.

The torque coupling drive mode can meet the operating conditions with high requirement of torque, and its power flow is shown in Fig 3(a), the speed and torque relationship between the input and output shaft is expressed as,

$$\begin{cases} n_3 = n_{\mathrm{in}1}/i_{\mathrm{g}1} \\ n_{\mathrm{in}2} = n_{\mathrm{in}1} i_{\mathrm{g}2}/i_{\mathrm{g}1} \\ T_3 = T_{\mathrm{in}1} i_{\mathrm{g}1} + T_{\mathrm{in}2} i_{\mathrm{g}2} \end{cases} \tag{5}$$

where $n_{\mathrm{in}1}$, $n_{\mathrm{in}2}$ and n_3 are the speed of input shaft 1, input shaft 2 and shaft 3 respectively, $T_{\mathrm{in}1}$, $T_{\mathrm{in}2}$ and T_3 are the torque of input shaft 1, input shaft 2 and shaft 3 respectively, $i_{\mathrm{g}1}$ and $i_{\mathrm{g}2}$ are the gear ratio.

According to the structure shown in Fig 2, if shaft 1 is connected to the engine and shaft 2 is connected to the motor, and $i_{\mathrm{g}1} = i_{\mathrm{g}2} = 1$ then the speed and torque of shaft 3 are $n_3 = n_{\mathrm{e}} = n_{\mathrm{m}}$ and $T_3 = T_{\mathrm{e}} + T_{\mathrm{m}}$, the above speed and torque relationship for torque coupling mode can also satisfied with pure electric drive mode and pure engine drive mode.

The speed coupling drive mode can expand the speed range of the tractor by the speed regulation capability of the motor, its power flow is shown in Fig 3(b), the speed and torque

TABLE 2. **Parameters of hydraulic components.**

Model	Rated displacement (cm^3/r)	Rated speed (r/min)	Maximum pressure difference (bar)	Torque (N·m/bar)	Flow rate (L/min)
055-VDP	55	3900	480	0.88	215
055-FDM	55	3900	480	0.88	215

TABLE 3. Element engagement status of each drive mode.

Drive modes	C1	C2	C3	B1
Pure electric drive (1)		▲		▲
Pure engine drive (2)	▲			▲
Torque coupling drive (3)	▲	▲		▲
Speed coupling drive (4)	▲		▲	

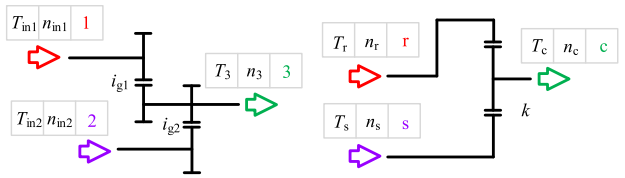

(a) Torque coupling (b)Speed coupling

FIGURE 3. Power flow of coupling mode.

relationship is expressed as,

$$\begin{cases} n_c = n_s/(1+k) + kn_r/(1+k) \\ T_r = kT_s \\ T_c = (1+k)T_r \end{cases} \tag{6}$$

where s, r, and c are the sun gear, ring gear, and carrier respectively. k is the characteristic parameter of the planetary gear set. n_c, n_s and n_r are the speed of carrier, sun gear, and ring gear respectively. T_r, T_s and T_c are the torque of ring gear, sun gear, and carrier respectively.

According to the structure shown in Fig 2, if the carrier is connected to the engine and sun gear is connected to the motor, then the speed and torque of ring gear is,

$$\begin{cases} n_r = [(1+k)n_e - n_m]/k \\ T_r = kT_m = T_e/(1+k) \end{cases} \tag{7}$$

B. TRANSMISSION MODES AND SPEED CHARACTERISTICS ANALYSIS

The MEH-PS has three transmission modes, which can be realized by controlling C4, B1, B2, and B3 for hydrostatic transmission mode, hydro-mechanical transmission mode, and mechanical transmission mode.

According to Fig 2, the speed relations can be described as,

$$\begin{cases} n_{c1} = n_{in} \quad n_{r1} = n_{r2} \\ \dfrac{n_{in}}{n_P} = -i_1 \quad \dfrac{n_M}{n_P} = e \quad \dfrac{n_M}{n_{s2}} = -i_2 \end{cases} \tag{8}$$

where n_{c1} is the carrier speed of the 1st planetary gear set, the subsequent speed and torque of the other planetary gears are named in the same way. n_{in} is the speed of input shaft, n_P, n_M is the speed of VDP and FDM respectively.

The relationship of the speed between each element of the planetary gear is as follows:

$$n_s + kn_r - (1+k)n_c = 0 \tag{9}$$

If C4 and B2 are engaged, $n_{r2} = 0$, According to Eq (8) and Eq (9), the speed relationship of hydrostatic transmission mode can be described as,

$$n_{c2} = \frac{en_{in}}{i_1 i_2 (1+k_2)} \tag{10}$$

If C4 and B1 are engaged, $n_{s1} = 0$, According to Eq (8) and Eq (9), the speed relationship of hydro-mechanical transmission mode can be described as,

$$n_{c2} = \frac{ek_1 n_{in} + k_2 i_1 i_2 (1+k_1) n_{in}}{i_1 i_2 k_1 (1+k_2)} \tag{11}$$

If B1 and B3 are engaged, $n_{s1} = n_{s2} = 0$, The speed relationship of mechanical transmission mode can be described as,

$$n_{c2} = \frac{k_2(1+k_1)n_{in}}{k_1(1+k_2)} \tag{12}$$

The sub-transmission consists of planetary gears K3 and K4 as well as clutch C5 and brakes B4 and B5. Engaging any of the shift elements can form a gear with a fixed transmission ratio. The function of sub-transmission is to expand the transmission ratio, which can realize the power demand of low speed and high speed at the same time; another function is to achieve synchronous shift between hydrostatic transmission mode and hydro-mechanical transmission mode, thus to realize the expansion of transmission ratio.

The ratio of sub-transmission is defined as,

$$i_{st} = \frac{n_{c2}}{n_{out}} \tag{13}$$

According to Fig 2, the speed relations of the sub-transmission is obtained as,

$$\begin{cases} n_{c3} = n_{c4} \\ n_{r4} = n_{out} \\ n_{r3} = n_{s4} = n_{c2} \end{cases} \tag{14}$$

According to Eqs (10), (14), and (15), if C5 is engaged then $n_{r3} = n_{s3}$, $i_{st} = 1$; if B4 is engaged, then $n_{s3} = 0$, $i_{st} = \frac{k_4(1+k_3)}{k_3 k_4 - 1}$; if B5 is engaged, then $n_{c4} = 0$, $i_{st} = -k_4$.

Each of the above transmission modes theoretically has three gears, which are matched to obtain the transmission ratio between the input and output shafts of each gear is shown in Table 4.

Where F is forward gear, R is reverse gear, H is hydrostatic transmission, M is mechanical transmission, HM is hydro-mechanical transmission; i_g is the transmission ratio of HMT.

Table 5 shows the parameters of each transmission element based on the relevant computation.

The above parameters are substituted into each transmission ratio to obtain the curve of transmission ratio about displacement ratio shown in Fig 4.

The speed relationship of speed coupling drive mode is related to the engine speed, the motor speed, the hydraulic system displacement ratio, and the sub-transmission ratio.

TABLE 4. Element engagement status and transmission ratio of each gear.

Transmission modes	Gear	C4	C5	B1	B2	B3	B4	B5	i_g
Hydrostatic transmission	F(H)	▲			▲			▲	$-\frac{i_1 i_2 k_4 (1+k_2)}{e}$
	R(H1)	▲			▲		▲		$\frac{i_1 i_2 k_4 (1+k_2)(1+k_3)}{e(k_3 k_4 - 1)}$
	R(H2)	▲	▲		▲				$\frac{i_1 i_2 (1+k_2)}{e}$
Hydro-mechanical	F (HM1)	▲		▲			▲		$\frac{i_1 i_2 k_1 k_4 (1+k_2)(1+k_3)}{[k_1 e + k_2 i_1 i_2 (1+k_1)](k_3 k_4 - 1)}$
	F (HM2)	▲	▲	▲					$\frac{i_1 i_2 k_1 (1+k_2)}{k_1 e + k_2 i_1 i_2 (1+k_1)}$
	R(HM)	▲		▲				▲	$-\frac{k_1 k_4 (1+k_2)}{k_2 (1+k_1)}$
Mechanical transmission	F (M1)			▲		▲	▲		$\frac{k_1 k_4 (1+k_2)(1+k_3)}{k_2 (1+k_1)(k_3 k_4 - 1)}$
	F (M2)		▲	▲		▲			$\frac{k_1 (1+k_2)}{k_2 (1+k_1)}$
	R(M)			▲		▲		▲	$-\frac{k_1 k_4 (1+k_2)}{k_2 (1+k_1)}$

TABLE 5. Transmission element parameters.

parameters	k_1	k_2	k_3	k_4	i_1	i_2
Value	1.80	1.60	1.65	1.65	0.62	1.00

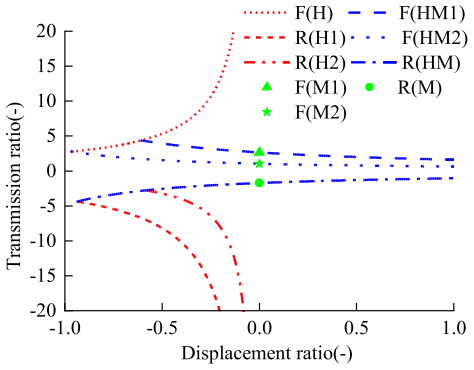

FIGURE 4. Characteristic curve of speed regulation of HMT.

According to Eqs (7), (8), (9) and (13), the output shaft speed of speed coupling drive mode can be described as,

$$n_{\text{out}} = \frac{ek_1 n_{\text{e}} + k_2 i_1 i_2 [(1+k_1) n_{\text{e}} + n_{\text{m}}]}{k_1 i_1 i_2 (1+k_2) i_{\text{st}}} \tag{15}$$

The step-less speed regulation is an important characteristic of MEH-PS. Fig 5 shows the speed curves of the

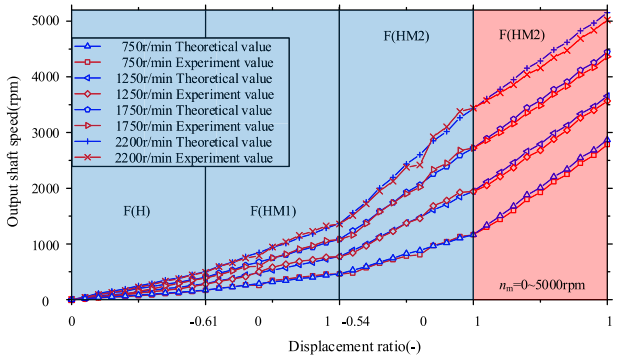

FIGURE 5. Step-less speed regulation characteristics under different input engine speeds.

transmission output shaft under different engine input speeds, where the blue area is the pure engine drive mode. When the engine speed is fixed, the transmission output shaft speed varies continuously with the change of displacement ratio, and the engine speed fluctuation makes the experiment data deviate partially from the theoretical data, however, it does not affect the conclusion. The red area is the speed coupling drive mode, this area is the transmission output shaft speed relationship when the displacement ratio of gear F (HM2) is $e = 1$. Since the engine speed and displacement ratio are fixed values, the increase of output shaft speed is achieved by the motor speed regulation, the figure shows the output shaft

speed of the motor speed increases from 0 to −5000rpm, there is an error between the theoretical and experiment values, but it's within the 5%, therefore the theoretical and experimental values of the transmission output speed are in good consistency. Speed coupling drive mode expands the transmission's range of speed regulation for higher tractor speed when the transmission ratio is limited.

C. TORQUE CHARACTERISTICS ANALYSIS

According to Fig 2, the torque relations can be described as,

$$\begin{cases} T_{c2} = T_{out}/i_{st} & T_{r1} = T_{r2} \\ T_e = T_{c1} + T_P/i_1 & T_P/T_M = e \quad T_{s2}/T_M = -i_2 \end{cases} \tag{16}$$

where T_{out} is the torque of the transmission output shaft and T_P/T_M is the pump/motor torque.

The relationship of the torque between each element of the planetary gear is as follows:

$$T_s = \frac{T_r}{k} = -\frac{T_c}{1+k} \tag{17}$$

According to Eqs (17) and (18) the input shaft torque of the hydrostatic transmission mode is:

$$T_{in} = \frac{T_P}{i_1} = \frac{eT_{out}}{i_1 i_2 i_{st}(1+k_2)} \tag{18}$$

The input shaft torque of the hydro-mechanical transmission mode is:

$$T_{in} = T_{c1} + \frac{T_P}{i_1} = \left(\frac{k_2(1+k_1)}{k_1} + \frac{e}{i_1 i_2}\right)\frac{T_{out}}{i_{st}(1+k_2)} \tag{19}$$

The input shaft torque of the mechanical transmission mode is:

$$T_{in} = T_{c1} = \frac{k_2(1+k_1)T_{out}}{k_1(1+k_2)i_{st}} \tag{20}$$

Taking the engine speed of 1500rpm as an example, the torque variation of the input shaft under different transmission output shaft torque is analyzed, and the torque relationship curve is shown in Fig 6. The blue area is the pure engine drive mode and the red area is the torque coupling drive mode. The maximum output torque of the engine is 750N·m, the maximum output torque of the motor is 250N·m, and the maximum output torque of the torque coupling drive mode is 1000N·m. From the figure, it shows that under the same torque, the input torque required in low-gear is smaller than that required in high-gear, and the higher the gear, the smaller the maximum torque the transmission can withstand, and vice versa. Gear F (HM1) is suitable for high-load operation, and gear F (HM2) is suitable for low-load operation. Torque coupling drive mode has the ability of a low-power engine to complete high-power operation tasks to some extent.

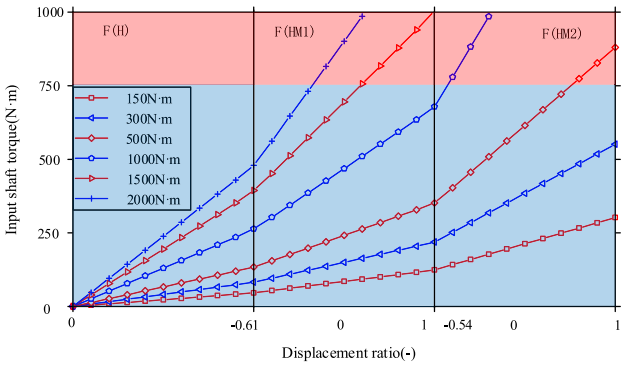

FIGURE 6. Torque characteristics under different loads.

D. POWER SPLIT AND EFFICIENCY CHARACTERISTICS ANALYSIS

The power split characteristic can be expressed as $\rho = P_H/P_I$, where P_H is the output power transferred by the hydraulic path (the input power of the sun gear of K2), P_I is the power of input shaft [28]. Fig 7 shows a simplified transmission chain.

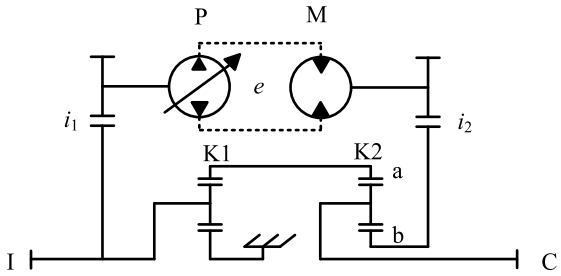

FIGURE 7. HMT closed drive circuit.

According to Eqs (9), (14), (17) and (21), it can be calculated that:

$$\rho = \frac{n_M T_M}{n_{in} T_{in}} = \frac{e}{i_1 i_2 k_2 (1+k_1)/k_1 + e} \tag{21}$$

The relationship between the inverse of the forward transmission ratio and the power split ratio $|\rho|$ shown in Fig 8 is obtained from the Eq (21), in which the transmission power split ratio is kept at a lower level, which is good for the efficiency of transmission.

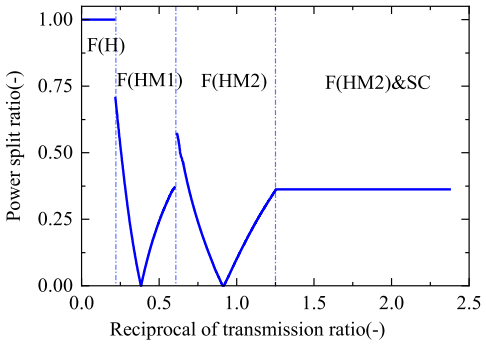

FIGURE 8. Hydraulic power split ratio curve.

For the 0-55 series VDP and FDM shown in Table 2, the efficiency expression was obtained by fitting the data

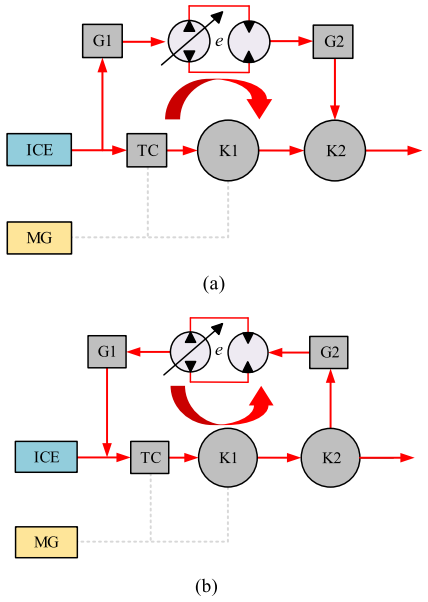

FIGURE 9. Normal power flow and circulating power flow.

obtained from a self-designed test bench as follows,

$$\eta_{\mathrm{P}} = 0.87[(\frac{n_{\mathrm{e}}}{i_1 n_{\mathrm{P\,max}}})^{0.05} + 0.035\sin(\frac{4n_{\mathrm{e}}}{i_1 n_{\mathrm{P\,max}}})] \times[\exp(\frac{-33T_{\mathrm{M}}}{D_{\mathrm{M\,max}}\Delta P_{\mathrm{P\,max}}}) - \exp(\frac{-50T_{\mathrm{M}}}{D_{\mathrm{M\,max}}\Delta P_{\mathrm{P\,max}}}) + \exp(\frac{0.5T_{\mathrm{M}}}{D_{\mathrm{M\,max}}\Delta P_{\mathrm{P\,max}}})]\,|e|^{0.5} \tag{22}$$

$$\eta_{\mathrm{M}} = 0.87[(\frac{en_{\mathrm{e}}}{i_1 n_{\mathrm{M\,max}}})^{0.05} + 0.035\sin(\frac{4en_{\mathrm{e}}}{i_1 n_{\mathrm{M\,max}}})] \times[\exp(\frac{-33T_{\mathrm{M}}}{D_{\mathrm{M\,max}}\Delta P_{\mathrm{M\,max}}}) - \exp(\frac{-50T_{\mathrm{M}}}{D_{\mathrm{M\,max}}\Delta P_{\mathrm{M\,max}}}) + \exp(\frac{0.5T_{\mathrm{M}}}{D_{\mathrm{M\,max}}\Delta P_{\mathrm{P\,max}}})] \tag{23}$$

where $n_{\mathrm{P\,max}}/n_{\mathrm{M\,max}}$ is the rated speed of the VDP/FDM; $D_{\mathrm{P\,max}}/D_{\mathrm{M\,max}}$ is the rated displacement of the VDP/FDM.

For the closed transmission chain consisting of the fixed shaft gear set and the planetary gear set, the transmission efficiency can be calculated by the gear meshing efficiency method [29], [30], and according to the structural relationship in Fig 7, the relevant ratio is calculated as,

$$\begin{cases} i_{\mathrm{aI}} = \dfrac{1+k_1}{k_1}\, i_{\mathrm{bI}} = \dfrac{e}{i_1 i_2}\; i^{\mathrm{b}}_{\mathrm{Ca}} = \dfrac{k_2}{1+k_2} \quad i^{\mathrm{a}}_{\mathrm{Cb}} = \dfrac{1}{1+k_2} \\ i^{\mathrm{a}}_{\mathrm{CI}} = i^{\mathrm{a}}_{\mathrm{Cb}} i_{\mathrm{bI}} = \dfrac{e}{i_1 i_2 (1+k_2)} \quad i^{\mathrm{b}}_{\mathrm{CI}} = i^{\mathrm{b}}_{\mathrm{Ca}} i_{\mathrm{aI}} = \dfrac{k_2(1+k_1)}{k_1(1+k_2)} \\ i_{\mathrm{CI}} = i^{\mathrm{a}}_{\mathrm{CI}} + i^{\mathrm{b}}_{\mathrm{CI}} = \dfrac{ek_1 + k_2(1+k_1) i_1 i_2}{(1+k_2) i_1 i_2 k_1} \\ i_{\mathrm{IC}} = \dfrac{1}{i_{\mathrm{CI}}} = \dfrac{1+k_2}{e/i_1 i_2 + k_2(1+k_1)/k_1} \end{cases} \tag{24}$$

where $i^{\mathrm{a}}_{\mathrm{CI}}$, $i^{\mathrm{b}}_{\mathrm{CI}}$ are the ratios of C to I when a and b are fixed, respectively.

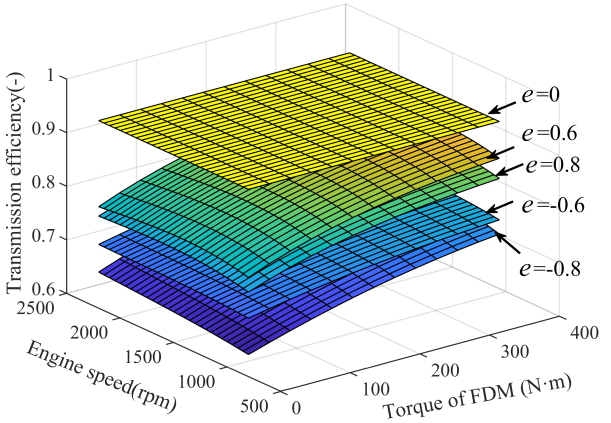

FIGURE 10. Transmission efficiency map.

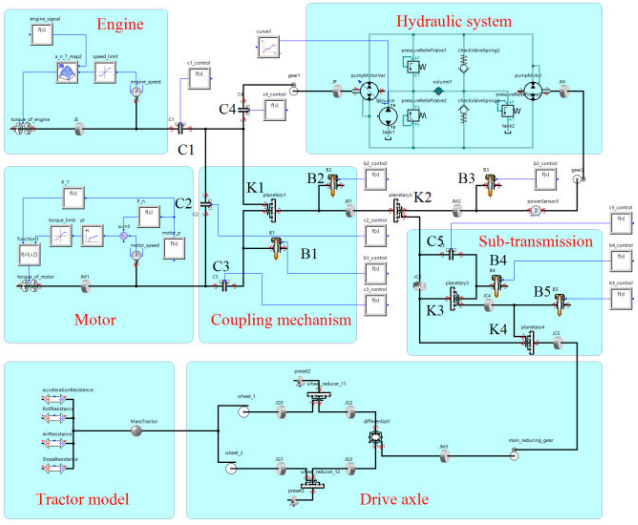

FIGURE 11. SimulationX model of the proposed MEH-PS.

If $e > 0$, $i^{\mathrm{a}}_{\mathrm{CI}} i^{\mathrm{b}}_{\mathrm{CI}} > 0$, as is shown in Fig 9(a), there is no circulating power in the closed transmission chain and the transmission efficiency is:

$$\eta_{\mathrm{t}} = \left\{1 + |i_{\mathrm{IC}}|\left[\left|i^{\mathrm{b}}_{\mathrm{CI}} - i^{\mathrm{b}}_{\mathrm{Ca}} i_{\mathrm{CI}}\right|\varphi + \left|i^{\mathrm{a}}_{\mathrm{CI}}\right|(1/\eta_{\mathrm{b}} - 1)\right]\right\}^{-1} \eta_{\mathrm{st}} \tag{25}$$

If $e < 0$, $i^{\mathrm{a}}_{\mathrm{CI}} i^{\mathrm{b}}_{\mathrm{CI}} < 0$, as is shown in Fig 9(b), there is circulating power in the closed transmission chain and the transmission efficiency is:

$$\eta_{\mathrm{t}} = \left\{1 + |i_{\mathrm{IC}}|\left[\left|i^{\mathrm{b}}_{\mathrm{CI}} - i^{\mathrm{b}}_{\mathrm{Ca}} i_{\mathrm{CI}}\right|\varphi + \left|i^{\mathrm{a}}_{\mathrm{CI}}\right|(1 - \eta_{\mathrm{b}})\right]\right\}^{-1} \eta_{\mathrm{st}} \tag{26}$$

where, φ is the planetary gear power loss coefficient, this paper takes 0.019, η_{b} is the efficiency of the b-I transmission chain, $\eta_{\mathrm{b}} = \eta_{i1}\eta_{\mathrm{P}}\eta_{\mathrm{M}}\eta_{i2}$, η_{st} is the efficiency of the sub-transmission. The meshing efficiency of the gear set is often regarded as a constant [31], the efficiency of the external-external gear set is 99%, and the efficiency of the internal-external gear set is 99.5%.

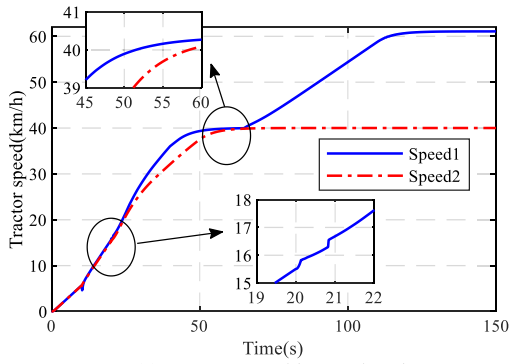

(a) Tractor speed in acceleration

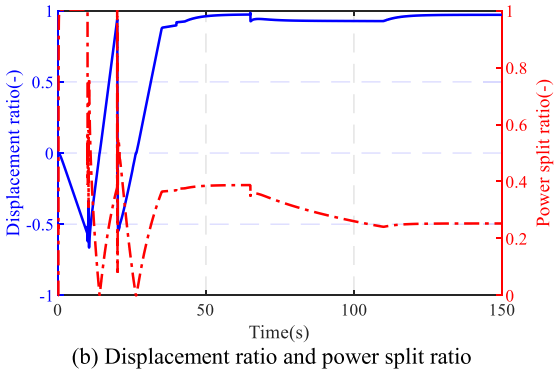

(b) Displacement ratio and power split ratio

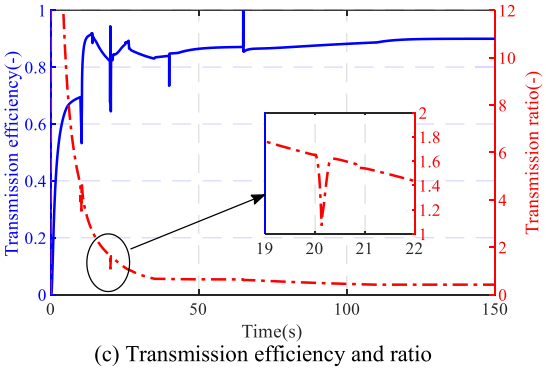

(c) Transmission efficiency and ratio

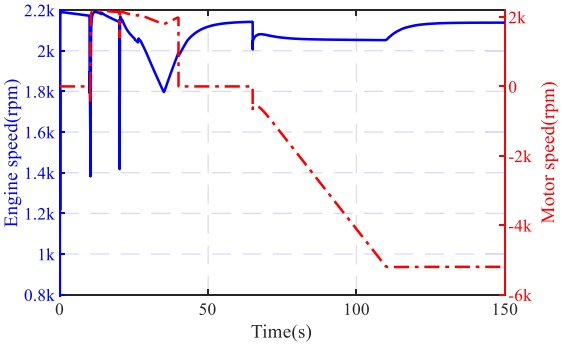

(d) Engine and motor speed

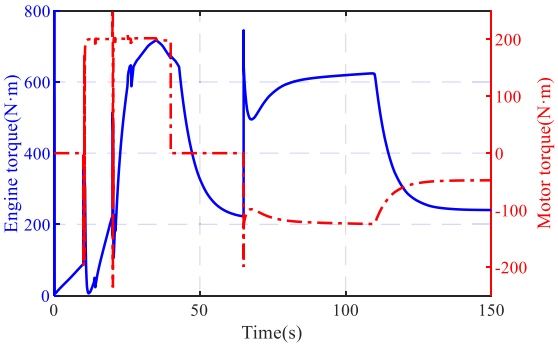

(e) Engine and motor torque

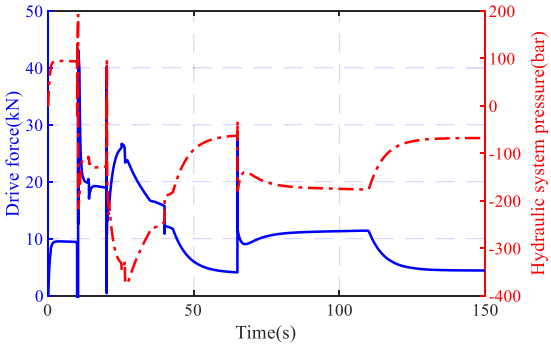

(f) Tractor driving force and hydraulic system pressure

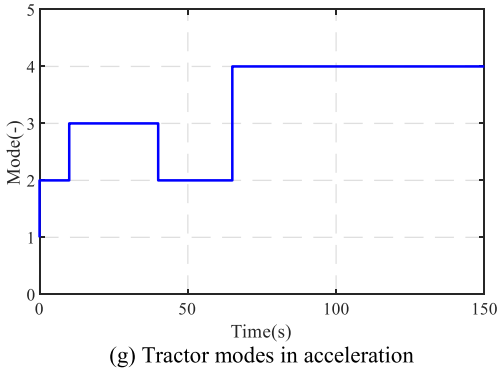

(g) Tractor modes in acceleration

FIGURE 12. **Performance simulation results.**

Substituting Eq (25) into Eqs (26) and (27) to obtain the transmission efficiency shown in Fig 10.

Fig 10 shows that if $|e|$ is equal, the efficiency corresponding to the normal power flow is significantly higher than the efficiency corresponding to the circulating power flow, and the smaller the $|e|$, the higher the efficiency, and the highest transmission efficiency is achieved when $e = 0$, the reason is that no power is transmitted through the hydraulic system, so the transmission energy loss is minimal. In addition, the larger the load torque of the hydraulic motor, the higher the efficiency of the transmission, to ensure higher efficiency of the transmission, the hydraulic system should avoid working in low load conditions.

IV. SIMULATION AND TEST

A. SIMULATION MODELING

According to the structure of MEH-PS shown in Fig 2 and the gear switching logic shown in Table 3 and Table 4, the simulation model of the whole tractor shown in Fig 11 was established in SimulationX. Because the acceleration process of full load transport requires high tractor traction and speed, it provides a valuable test condition for the performance of the tractor equipped with the MEH-PS [16], [21]. The tractor operation mass is 8260kg, the mass of cargo and trailer is 16440kg, the total mass of the tractor is 26350kg, the axle ratio is 23.68, the tire rolling radius is 0.75m.

B. SIMULATION RESULTS IN ACCELERATION CONDITION

The simulation results of the acceleration process of the tractor equipped with MEH-PS for full load transport are shown in Fig 12. Speed 1 and speed 2 in Fig 12(a) are the speed comparison of the tractor with motor-assisted (tractor 1) and tractor (tractor 2) without motor-assisted. Under the same shift conditions and engine throttle opening, the tractor speed increased from 0 to 40km/h, tractor 1 reached the speed in 58.6s and tractor 2 reached the speed in 51.5s. The acceleration results of 0∼40km/h indicate that the tractor has better acceleration performance and dynamics in the torque coupling mode.

It is worth noting that in Fig 12(b), when switching from gear F (HM1) to gear F (HM2) at the moment of 20s, the displacement ratio changed instantaneously in steps and the transmission ratio decreased slightly, but it had no significant effect on the tractor speed because of the large vehicle inertia when the tractor was fully loaded. In addition, the gear or mode switching was also undertaken at the moments of 10s, 40s and 65s, and the vehicle drive force changed abruptly at the time of switching, but the relevant parameters of the engine, motor, and hydraulic system changed within an accepted range.

The tractor switched to speed coupling drive mode in 65s, the speed increased from 40km/h to 60km/h in 65s∼120s, the motor speed reached −5200rpm then, the speed increase was achieved through the motor speed regulation, but the acceleration of the tractor is smaller compared to the acceleration of 0∼40km/h, which is the difference between speed coupling and torque coupling drive, expanding the speed range but lose some of the acceleration ability. In Fig 12(b), although the displacement ratio of the hydraulic system remains basically unchanged during the acceleration of 40∼60 km/h, the power split ratio decreases, which has a deviation from the theoretical analysis results in Fig 8. The reason is that the proportion of the output power of the motor gradually increases during the acceleration process, so that the proportion of the output power of the hydraulic system decreases, and the power split ratio remains constant at the end of the acceleration, which is consistent with the real case. The efficiency of the transmission increases and this is related to the decrease of the hydraulic power split ratio, and the efficiency of the transmission in Fig 12(c) remains mostly above 86%.

Fig 12(g) shows that the accelerating process of the tractor only experienced four shifts to increase the speed from 0 to 60km/h. Compared to conventional tractors equipped with stepped transmissions [32], the number of gear shifts is less, which is beneficial to the service life and driving comfort of the tractor. In Fig 12(d), 12(e) and 12(f), according to the parameters shown in Table 1 and Table 2, the speed and torque of the power source and oil pressure of the hydraulic system during the operation of the tractor are within its permissible parameters, and the designed MEH-PS can meet the requirements of tractor transport.

C. BENCH TEST

The test bench shown in Fig 13 is built according to the structural principle of Fig 14 of the MEH-PS, and the power of the traction motor (simulated engine) and the drive motor are combined to drive the transmission through the coupling mechanism, and the performance of the powertrain system can be tested by loading on the dynamometer with the control of the load torque. The parameters of the test bench were shown in Table 5.

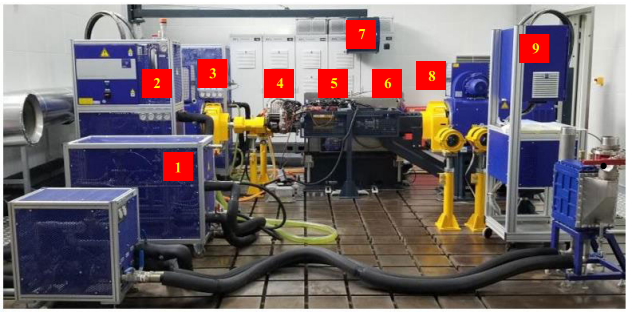

FIGURE 13. MEH-PS test bench. 1. Oil cooling system 2. Motor cooling system 3. Traction motor 4. Drive motor and coupling mechanism 5. HMT 6. Reduction gear 7. Power cabinet of dynamometer 8. Electrical dynamometer 9. Controller cabinet.

Fig 15 shows the comparison of the results about the simulation and experiment transmission ratio, the figure shows the ratio in the range of 0.41∼12. When the tractor speed is low, the ratio slope changes greatly, and the tractor can get

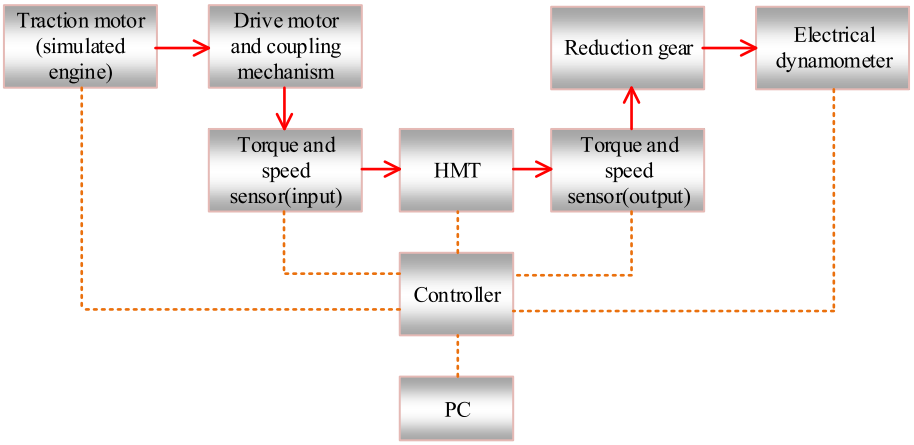

FIGURE 14. Test bench operating principle.

TABLE 6. Parameters of the test bench.

Components	Specifications
Traction motor	Rated power: 500kW Rated torque: 1250 N·m
Electrical dynamometer	Rated power: 1000kW Rated torque: 2900 N·m
Torque and speed sensor	Range：0~5000Nm; 0~8000r/min Accuracy：±0.05%

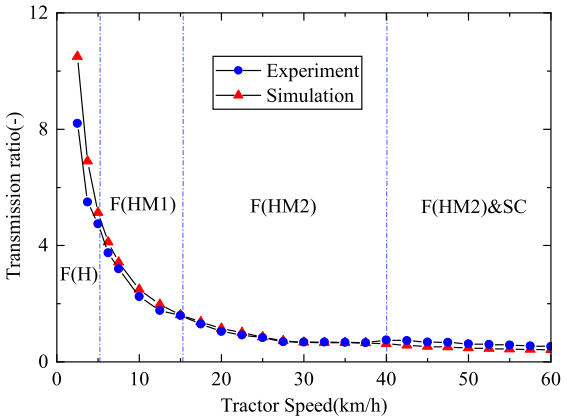

FIGURE 15. Simulation and experiment transmission ratio.

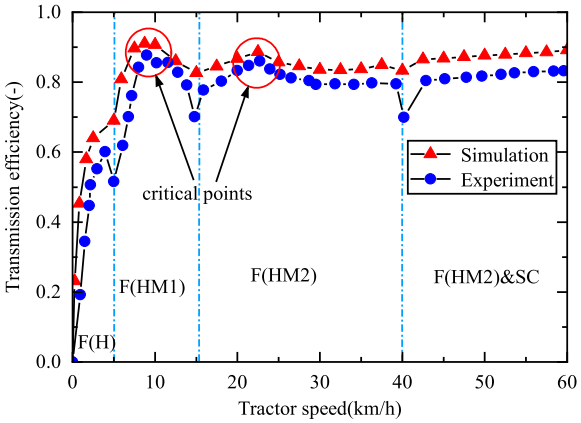

FIGURE 16. Simulation and experiment transmission efficiency.

more acceleration at a low speed. When the speed is less than 5.6km/h, the difference between simulation and experiment data is larger due to gear F (H) is hydrostatic transmission, and the leakage of the hydraulic system has a greater impact on the transmission ratio.

Fig 16 shows the comparison between simulation and experiment of transmission efficiency. There are two local highest efficiency critical points on the curve, both of which are the efficiency of mechanical transmission gears, and the experiment efficiency is lower than the simulated efficiency, which is attributed to the simplification of the simulation modeling. In addition, the efficiency of the experiment is significantly smaller than that of the simulation during mode switching because the simulation modeling considers only the transient effect and does not consider the energy loss of the shift element during the switching process. The results of the experiment and simulation are in good consistency overall.

V. CONCLUSION

In this paper, according to the characteristics of current mainstream drive and transmission technologies, a MEH-PS integrating electromechanical hybrid system and hydro-mechanical composite transmission is proposed to meet the operational requirements of the tractor. The scheme conception and structure design are completed, and the power sources and transmission components are selected according to the relevant work content of the tractor. The drive and transmission principles of the powertrain are discussed. The speed characteristics, torque characteristics, power split, and efficiency characteristics of the proposed system are theoretically analyzed. The simulation model of the whole tractor

is established in SimulationX, and the acceleration process of full load transport is taken as the object of the study. The results show that the tractor equipped with MEH-PS has better dynamics and a wider speed range compared with the conventional tractor while maintaining a high transmission efficiency, and the selected power sources and transmission components are within the permitted parameters, which verifies the reliability of the scheme. Compare the simulation and experiment results found that: Although there are differences between the simulated and experimental data on speed regulation characteristics and efficiency characteristics in the tractor speed range, the overall is in good agreement, which confirms the advantages of the scheme in terms of speed regulation and efficiency performance. The powertrain can also apply to a loader, grader, and other vehicles, which has a relatively wide application prospect.

REFERENCES

[1] J. Yu, Z. Cao, M. Cheng, and R. Pan, "Hydro-mechanical power split transmissions: Progress evolution and future trends," *Proc. Inst. Mech. Eng., D, J. Automobile Eng.*, vol. 233, no. 3, pp. 727–739, Feb. 2019.

[2] A. Rossetti and A. Macor, "Continuous formulation of the layout of a hydromechanical transmission," *Mechanism Mach. Theory*, vol. 133, pp. 545–558, Mar. 2019.

[3] J. Wang, Y. Cai, L. Chen, D. Shi, R. Wang, and Z. Zhu, "Review on multi-power sources dynamic coordinated control of hybrid electric vehicle during driving mode transition process," *Int. J. Energy Res.*, vol. 44, no. 8, pp. 6128–6148, Jun. 2020.

[4] W. Du, S. Zhao, L. Jin, J. Gao, and Z. Zheng, "Optimization design and performance comparison of different powertrains of electric vehicles," *Mechanism Mach. Theory*, vol. 156, Feb. 2021, Art. no. 104143.

[5] M. Simikić, N. Dedović, L. Savin, M. Tomić, and O. Ponjičan, "Power delivery efficiency of a wheeled tractor at oblique drawbar force," *Soil Tillage Res.*, vol. 141, pp. 32–43, Aug. 2014.

[6] T. Jokiniemi, A. Suokannas, and J. Ahokas, "Energy consumption in agriculture transportation operations," *Eng. Agricult., Environ. Food*, vol. 9, no. 2, pp. 171–178, Apr. 2016.

[7] B. Li, D. Sun, M. Hu, X. Zhou, D. Wang, Y. Xia, and Y. You, "Automatic gear-shifting strategy for fuel saving by tractors based on real-time identification of draught force characteristics," *Biosyst. Eng.*, vol. 193, pp. 46–61, May 2020.

[8] W. Chancellor and N. Thai, "Automatic control of tractor transmission ratio and engine speed," *Trans. ASAE*, vol. 27, no. 3, pp. 642–646, 1984.

[9] F. Wang, M. A. Mohd Zulkefli, Z. Sun, and K. A. Stelson, "Energy management strategy for a power-split hydraulic hybrid wheel loader," *Proc. Inst. Mech. Eng., D, J. Automobile Eng.*, vol. 230, no. 8, pp. 1105–1120, Jul. 2016.

[10] K. T. Renius and R. Resch, *Continuously Variable Tractor Transmissions*. St. Joseph, MI, USA: American Society of Agricultrual Engineers, 2005.

[11] Y. Xia and D. Sun, "Characteristic analysis on a new hydro-mechanical continuously variable transmission system," *Mechanism Mach. Theory*, vol. 126, pp. 457–467, Aug. 2018.

[12] Z. Zhu, X. Gao, L. Cao, Y. Cai, and D. Pan, "Research on the shift strategy of HMCVT based on the physical parameters and shift time," *Appl. Math. Model.*, vol. 40, nos. 15–16, pp. 6889–6907, Aug. 2016.

[13] F. Brumercik, R. Kocur, M. Pazican, and M. Lukac, "Differential hydro-mechanical transmissions with hydrostatic units," *Commun.-Sci. Lett. Univ. Zilina*, vol. 7, no. 1, pp. 49–53, 2005.

[14] W. Wu, J. Luo, C. Wei, H. Liu, and S. Yuan, "Design and control of a hydro-mechanical transmission for all-terrain vehicle," *Mechanism Mach. Theory*, vol. 154, Dec. 2020, Art. no. 104052.

[15] A. Rossetti and A. Macor, "Multi-objective optimization of hydro-mechanical power split transmissions," *Mechanism Mach. Theory*, vol. 62, pp. 112–128, Apr. 2013.

[16] F. Liu, W. Wu, J. Hu, and S. Yuan, "Design of multi-range hydro-mechanical transmission using modular method," *Mech. Syst. Signal Process.*, vol. 126, pp. 1–20, Jul. 2019.

[17] G. Wang, Y. Song, J. Wang, M. Xiao, Y. Cao, W. Chen, and J. Wang, "Shift quality of tractors fitted with hydrostatic power split CVT during starting," *Biosyst. Eng.*, vol. 196, pp. 183–201, Aug. 2020.

[18] C. Mansour and D. Clodic, "Dynamic modeling of the electro-mechanical configuration of the Toyota Hybrid System series/parallel power train," *Int. J. Automot. Technol.*, vol. 13, no. 1, p. 143, 2012.

[19] P. Joshi and V. Kartik, "Comparative analysis of the speed coupling and torque coupling hybrid modes of a parallel hybrid electric mini truck," in *Mechanism and Machine Science*. Springer, 2021, pp. 585–599. [Online]. Available: https://link.springer.com/chapter/10.1007/978-981-15-4477-4_42

[20] Y. Gao and M. Ehsani, "A torque and speed coupling hybrid drivetrain-architecture, control, and simulation," *IEEE Trans. Power Electron.*, vol. 21, no. 3, pp. 741–748, May 2006.

[21] F. Mocera and A. Somà, "Analysis of a parallel hybrid electric tractor for agricultural applications," *Energies*, vol. 13, no. 12, p. 3055, Jun. 2020.

[22] G. P. Moreda, M. A. Muñoz-García, and P. Barreiro, "High voltage electrification of tractor and agricultural machinery—A review," *Energy Convers. Manage.*, vol. 115, pp. 117–131, May 2016.

[23] Y. Xia, D. Sun, D. Qin, and W. Hou, "Study on the design method of a new hydro-mechanical continuously variable transmission system," *IEEE Access*, vol. 8, pp. 195411–195424, 2020.

[24] C.-Y. Li and G.-P. Liu, "Optimal fuzzy power control and management of fuel cell/battery hybrid vehicles," *J. Power Sources*, vol. 192, no. 2, pp. 525–533, 2009.

[25] S. K. Pitla, J. D. Luck, J. Werner, N. Lin, and S. A. Shearer, "In-field fuel use and load states of agricultural field machinery," *Comput. Electron. Agricult.*, vol. 121, pp. 290–300, Feb. 2016.

[26] B. Carl, M. Ivantysynova, and K. Williams, "Comparison of operational characteristics in power split continuously variable transmissions," SAE Tech. Paper 2006-01-3468, Oct. 2006.

[27] Q. Zhang, X. Kong, B. Yu, K. Ba, Z. Jin, and Y. Kang, "Review and development trend of digital hydraulic technology," *Appl. Sci.*, vol. 10, no. 2, p. 579, Jan. 2020.

[28] M. I. Ramdan, "Optimal design of a hydro-mechanical transmission power split hybrid hydraulic bus," Univ. Minnesota, Minneapolis, MN, USA, Tech. Rep. 3607931, 2013. [Online]. Available: https://conservancy.umn.edu/handle/11299/162514

[29] A. K. Gupta and C. P. Ramanarayanan, "Analysis of circulating power within hybrid electric vehicle transmissions," *Mechanism Mach. Theory*, vol. 64, pp. 131–143, Jun. 2013.

[30] T. Xie, J. Hu, Z. Peng, and C. Liu, "Synthesis of seven-speed planetary gear trains for heavy-duty commercial vehicle," *Mechanism Mach. Theory*, vol. 90, pp. 230–239, Aug. 2015.

[31] P. Dong, Y. Liu, P. Tenberge, and X. Xu, "Design and analysis of a novel multi-speed automatic transmission with four degrees-of-freedom," *Mech. Mach. Theory*, vol. 108, pp. 83–96, Feb. 2017.

[32] B. Li, D. Sun, M. Hu, X. Zhou, J. Liu, and D. Wang, "Coordinated control of gear shifting process with multiple clutches for power-shift transmission," *Mechanism Mach. Theory*, vol. 140, pp. 274–291, Oct. 2019.

ZHEN ZHU (Member, IEEE) received the B.S., M.S., and Ph.D. degrees from the School of Automotive and Traffic Engineering, Jiangsu University, Zhenjiang, China, in 2009, 2013, and 2016, respectively. In 2016, he joined the Automotive Engineering Research Institute, Jiangsu University, as an Assistant Professor. His research interests include artificial intelligence, vehicle dynamics, and control theory.

LONGHUI LAI (Member, IEEE) was born in Ganzhou, Jiangxi, China, in 1997. He received the B.S. degree in vehicle engineering from Northeast Forestry University, Harbin, China, in 2019. He is currently pursuing the M.Sc. degree with Jiangsu University, Zhenjiang, China. His current research interests include hybrid powertrain design and control and theoretical design of hydro-mechanical transmissions.

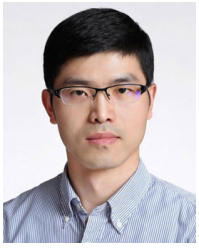

XIAODONG SUN (Senior Member, IEEE) received the B.Sc. degree in electrical engineering and the M.Sc. and Ph.D. degrees in control engineering from Jiangsu University, Zhenjiang, China, in 2004, 2008, and 2011, respectively. Since 2004, he has been with Jiangsu University, where he is currently a Professor in vehicle engineering with the Automotive Engineering Research Institute. His current teaching and research interests include electrified vehicles, electrical machines, electrical drives, and energy management. He is an Editor of the IEEE TRANSACTIONS ON ENERGY CONVERSION.

LONG CHEN (Member, IEEE) was born in Jingjiang, Jiangsu, China, in 1958. He received the B.S. and Ph.D. degrees in mechanical engineering from Jiangsu University, Zhenjiang, China, in 1982 and 2006, respectively. He is currently a Professor with the Automotive Engineering Research Institute, Jiangsu University. His research interests include electric vehicles, electric drives, simulation and control of vehicle dynamic performance, vehicle operation, and transport planning.

YINGFENG CAI (Member, IEEE) was born in Nantong, Jiangsu, China, in 1985. She received the B.S., M.S., and Ph.D. degrees from the School of Instrument Science and Engineering, Southeast University, Nanjing, China. In 2013, she joined the Automotive Engineering Research Institute, Jiangsu University, as an Assistant Professor. Her research interests include computer vision, intelligent transportation systems, and intelligent automobiles.